

Parallelization of Spectral Landau Fluid Code Using MPI

Masatoshi Yagi,* YoungWoo Cho,[†] Haruki Seto,* Taik Soo Hahm,[†]

*National Institutes for Quantum and Radiological Science and Technology, 2-166, Omotedate, Rokkasho, 039-3212, Japan

[†]Seoul National University, Department of Nuclear Engineering, 32-203, 599 Gwanak-ro, Gwanak-gu, Seoul 151-744, Korea
yagi.masatoshi@qst.go.jp

Abstract - 3-field Landau fluid code which is written by the spectral method is parallelized using Message Passing Interface. The calculation cost of nonlinear mode coupling is most expensive part, so that various schemes are tested to optimize it. It is found that the best scheme gives roughly 30% faster than the standard decomposition of do loop.

I. INTRODUCTION

3-field Landau fluid (LF3) model describes the ion temperature gradient driven drift wave (ITG) turbulence in Tokamak plasmas[1]. It is applied to investigate the internal transport barrier formation which gives the improved energy confinement time[2]. The code is developed using the spectral method[3] which is parallelized using Message Passing Interface (MPI)[4, 5]. Since the calculation cost of nonlinear mode coupling is most expensive part, so that various schemes for the decomposition of do loop are tested to optimize it. It is found that the best scheme gives roughly 30% faster than the standard decomposition method.

II. PARALLELIZATION

LF3 code is schematically written by

$$\frac{\partial f}{\partial t} = L(f) + N(f, f), \quad (1)$$

where f is the vector consist of the electrostatic potential fluctuation, the velocity fluctuation parallel to the ambient magnetic field and the ion temperature fluctuation, $L(f)$ represents linear term and $N(f, f)$ represents the convective nonlinearity which is expressed by the Poisson bracket. The predictor-corrector scheme[6] is adopted for time integration, namely

$$\frac{f^{n+1/2} - f^n}{\Delta t/2} = \frac{L(f^{n+1/2}) + L(f^n)}{2} + N(f^n, f^n), \quad (2)$$

and

$$\frac{f^{n+1} - f^n}{\Delta t} = \frac{L(f^{n+1}) + L(f^n)}{2} + N(f^{n+1/2}, f^{n+1/2}). \quad (3)$$

where the superscript indicates the each time step and the linear term is solved by Crank-Nicolson implicit scheme[7]. Figure 1 shows an example of Fourier spectrum in (m, n) space where m represents the poloidal mode number and n represents the toroidal mode number. It consists of resonant modes $q(r) = m/n$ and off-resonant modes. Here $q(r)$ represents the safety factor profile. The complex conjugate of these modes are also taken into account for the nonlinear mode coupling calculation. The resonant mode is given by:

REAL(DP),DIMENSION(2),PARAMETER:: &
SIG/(1.D0,-1.D0/)

```
DO LZ=1,KZM
DO LY=1,KYM
XRES=ABS(REAL(LZ)/REAL(LY))
IF(XRES.GT. 1/Q(0)*XKMSEL &
.OR. XRES.LT. 1/Q(IRMAX)/XKMSEL) THEN
CONTINUE
ELSE
DO LK=1,2
L=L+1
LKY(L)=LY
LKZ(L)=LZ*SIG(LK)
...
END DO
END DO
END DO
```

If we choose XKMSEL=1, it means only resonant modes are taken into account. In addition, we also include off-resonant modes such as the convective cell modes ($n = 0$). The nonlinear mode coupling table is constructed as

```
DO L=0,LMAX ! Parallel version: L=S,E
LX=0
DO L1=-LMAX,LMAX
DO L2=-LMAX,LMAX
MY=LKY(L)-LKY(L1)-LKZ(L2)
MZ=LKZ(L)-LKZ(L1)-LKZ(L2)
IF(MY.EQ. 0 .AND. MZ.EQ.0) THEN
LX=LX+1
LL1(L,LX)=L1
LL2(L,LX)=L2
ENDIF
END DO
END DO
LLMAX(L)=LX
END DO
```

Using the mode coupling table, the $E \times B$ nonlinearity is calculated by

```
DO L=S1,E1 ! Parallelization: Case IV
DO LL=1,LLMAX(L)
M1=LL1(L,LL)
M2=LL2(L,LL)
!$OMP PARALLEL DO
```

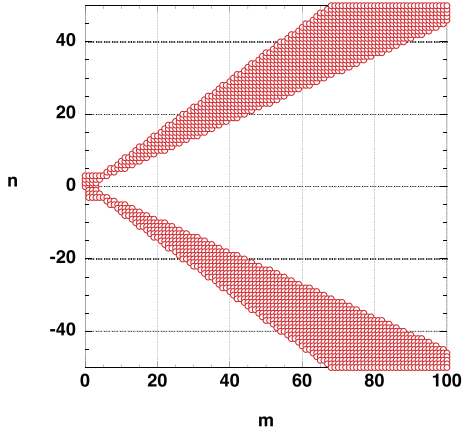


Fig. 1. An example of Fourier spectrum in (m, n) space.

```
DO I=1,IRMAXM
VOLRHS2(I,L)=VOLRHS(I,L)+ RHOS**2 &
*FKY(I,M1)*(VOLG(I,M1))*DPHIG(I,M2) &
-PHIG(I,M1)*DVOLG(I,M2))
...
END DO
!$OMP END PARALLEL DO
END DO
END DO
...
CALL MPI_ALLGATHER(VOLRHS2,COUNT2, &
MPI_DOUBLE_COMPLEX,VOLRHS(0,0),COUNTS2, &
DISP2, MPI_DOUBLE_COMPLEX, COMM1D,IERR)
```

Figure 2 shows a schematic view of number of non-linear mode coupling for each Fourier mode L . The four schemes are tested for the outer loop parallelization. In the case (I), the mode pointer L ($0 \leq L \leq LMAX$) which indicates the set of Fourier mode (m, n) is equally decomposed. In the case (II), the mode pointer is firstly divided by two groups, then, it is equally decomposed by different order. For the first group, each process is allocated as $0, 1, \dots, N$ and for the second group, it is allocated as $N, N-1, \dots, 0$. In the case (III), the one dimensional domain decomposition is applied. Initially, the domain decomposition gives $f^n(I, L)$, where $1 \leq I \leq IRMAX$ and $S \leq L \leq E$. Then, transpose of $f^n(I, L)$ is done to evaluate the nonlinear coupling, where $S \leq I \leq E$ and $0 \leq L \leq LMAX$. In this case, we need two MPI_ALLTOALL communications. In the case (IV), we calculate the total number of nonlinear mode coupling, then it is equally decomposed as much as possible.

Figure 3 shows the benchmark results of each scheme on PC cluster (VT64 Itanium 2 Server 2000 1.4GHz x 34 CPU, Myrinet). In this benchmark, 16 MPI processes are used for the benchmark test. Here ITG_NON2.DAT corresponds to case (I) (red circle), ITG_NON22.DAT, case (II) (blue triangle), ITG_NON23.DAT, case(III) (yellow square) and ITG_NON24.DAT, case (IV) (green reverse triangle). It is shown that the case (IV) is roughly 30% faster than the case (I).

To keep equal load balance on each process, we evaluate the total number of nonlinear mode coupling and it is divided

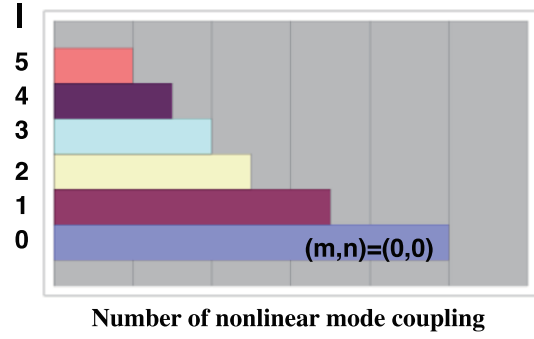


Fig. 2. A schematic view of number of nonlinear mode coupling for each Fourier mode L .

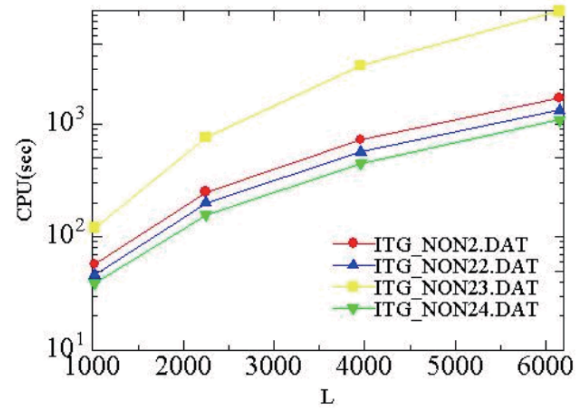


Fig. 3. The benchmark results of each scheme on PC cluster.

by total process number, then we search the neighbourhood of the value which is done by the following program:

```
LLMAX(0)=LLMAX(0)
DO L=1,LMAX
LLMAXS(L)=LLMAXS(L-1)+LLMAX(L)
END DO
LLTOT=0
DO L=0,LMAX
LLTOT=LLTOT+LLMAX(L)
END DO
LLAV=LLTOT/NUMPROCS
E2=1
DO I=0,NUMPROCS-2
DO L=0,LMAX
IF(LLMAXS(L)-E2+1 > LLAV) THEN
IF(I==0) THEN
LSE(I,1)=0
ELSE
LSE(I,1)=LSE(I-1,2)+1
END IF
IF(ABS(LLMAXS(L)-E2+1-LLAV) &
<= ABS(LLMAXS(L)-E2+1-LLAV)) THEN
LSE(I,2)=L-1
ELSE
LSE(I,2)=L

```

```

ENDIF
E2=LLMAXS(LSE(I,2))
EXIT
ENDIF
END DO
END DO
LSE(NUMPROCS-1,1)=LSE(NUMPROCS-2,2)+1
LSE(NUMPROCS-1,2)=LMAX
...
S1=LSE(MYID,1)
E1=LSE(MYID,2)

```

The nonlinear mode coupling table is also parallelized by MPI. It is benchmarked on IFERC-CSC HELIOS computer (BULL/Bullx B510: 2 processors of INTEL Sandy-Bridge EP 8 cores -2.7GHz). We use 16 node (256 process) for the benchmark test. For $LMAX = 15380$, the serial version gives roughly 3 hours to calculate nonlinear mode coupling table, however, the parallelized version gives only 93.5 second, it is quit efficient for large number of Fourier modes.

III. MPI/OPENMP HYBRID MODEL

The performance of threads is measured by fixing the process number. Japan Atomic Energy Agency (JAEA) supercomputer system (SGI ICE X: Intel Xeon E5-2680 v3) is used for the benchmark tests. Two cases with (A) $LMAX = 3890$ and (B) $LMAX = 9874$ are examined. For case (A), the process number is fixed as 256 processes and for (B), as 512 processes. In case with 4 threads, the factor 2 of performance

Case	1 thread	2 threads	4 threads
(A)	110.0 sec	65.3 sec	54.0 sec
(B)	324.8 sec	198.6 sec	160.6 sec

improvement is obtained. It is shown that MPI/OpenMP hybrid model is efficient way to improve the performance of LF3 code.

IV. EXAMPLE OF SIMULATION RESULT BY LF3

In this section, simulation results by LF3 are shown. The reversed q profile with $q(r = 0.6) = q_{min}$ is used. Figure 4 shows the heating source profiles. The Gaussian type of heating source profile is shown for the central ($P = 1$, $r_s = 0$, $\Delta = 0.2$) and off-axis ($P = 2$, $r_s = 0.4$, $\Delta = 0.05$) heating, where $S(r) = P \exp(-(r - r_s)^2/\Delta^2)$. Figure 5 shows the time evolution of ion temperature profile. The heating source is applied at $t = 2$ and the subsequent profile evolution is followed. It is seen that the internal transport barrier (ITB) forms at $r = 0.4$ for the off-axis heating.

Figure 6 shows the contour plot of temperature fluctuation at $t = 20$. The poloidal cross section with $\zeta = 0$ is shown. The strong intensity of temperature fluctuation indicates the location of heating source ($r = 0.4$). The large structure develops outside of ITB region.

To clarify the process of strong ITB formation, we should take account of the Shafranov shift which will be produced by the heating source. It is left as a future work.

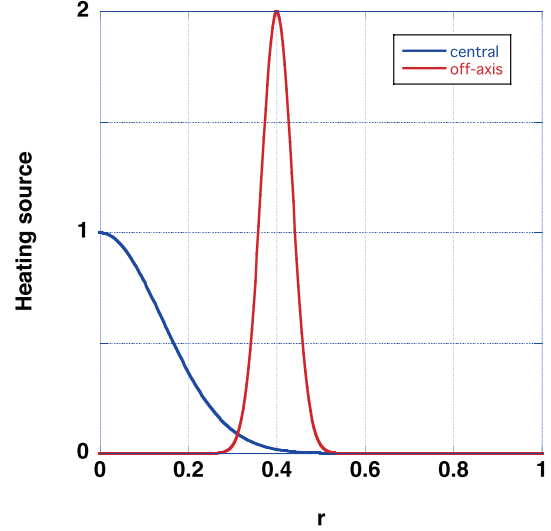


Fig. 4. The heating source profiles for central and off-axis heating.

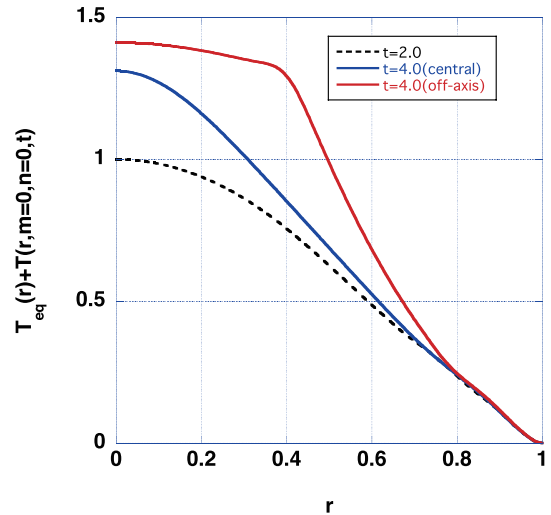


Fig. 5. The time evolution of ion temperature.

V. CONCLUSIONS

LF3 code is parallelized using MPI. We analyzed the cost of each subroutine and found that the calculation of nonlinear mode coupling is quite expensive. To keep equal load balance on each process, we calculate the total number of nonlinear mode coupling, then it is equally decomposed as much as possible. This method gives roughly 30% faster than the standard case where the total Fourier mode number $LMAX$ is simply divided by the total process number.

VI. ACKNOWLEDGMENTS

The numerical simulations were performed on the HELIOS supercomputer system at Computational Simulation Centre of International Fusion Energy Research Centre (IFERC-CSC, Aomori, Japan, under the Broader Approach collaboration between Euratom and Japan, implemented by

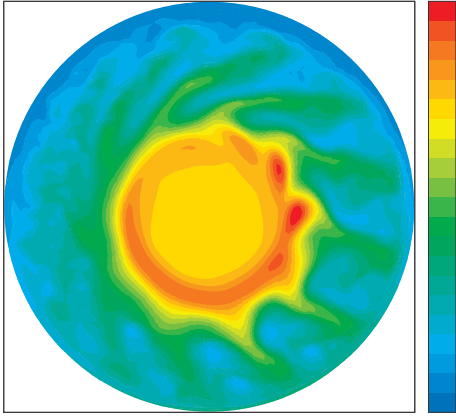


Fig. 6. The contour plot of ion temperature fluctuation at $t = 20$.

Fusion for Energy and QST). JAEA supercomputer system is also used for benchmark tests.

VII. NOMENCLATURE

f =field variable represented by $\{\phi, v, T\}$

ϕ =electrostatic potential fluctuation

v =parallel ion velocity fluctuation

T =ion temperature fluctuation

$\partial/\partial t$ =the partial time derivative

L =linear operator

N =nonlinear operator : $[\phi, f]$

$[\cdot, \cdot]$ =Poisson bracket

Δt =time step size

t =time

q =safety factor

r = minor radius of Tokamak

ζ =toroidal angle

REFERENCES

1. M. OTTAVIANI and G. MANFREDI, "The gyro-radius scaling of ion thermal transport from global numerical simulations of ion temperature gradient driven turbulence," *Physics of Plasmas*, **6**, 8, 3267 (1999).
2. S. TOKUNAGA, M. YAGI, S.-I. ITOH, and K. ITOH, "Multi-scale transport simulation of toroidal momentum source profile effect on internal transport barrier collapse," *Nuclear Fusion*, **49**, 075023 (2009).
3. C. CANUTO, M. HUSSAINI, A. QUARTERONI, and Z. T.A., *Spectral Methods in Fluid Dynamics*, Springer-Verlag, 1st ed. (1986).
4. W. GROPP, E. LUSK, and A. SKJELLUM, *Using MPI Portable Parallel Programming with the Message-Passing Interface*, The MIT Press, 3rd ed. (2014).
5. W. GROPP, T. HOEFLER, R. THAKUR, and E. LUST, *Using Advanced MPI Modern Features of the Message-Passing Interface*, The MIT Press (2014).
6. W. PRESS, S. TEUKOLSKY, W. VETTERLING, and B. FLANNERY, *NUMERICAL RECIPES in FORTRAN The Art of Scientific Computing*, Cambridge University Press, 2nd ed. (1992).

7. J. CRANK and P. NICOLSON, "A practical method for numerical evaluation of solutions of partial differential equations of the heat conduction type," *Proceedings Of The Cambridge Philosophical Society*, **43**, 1, 50 (1947).